Search for multi-atom resonant photoemission in magnetic thin films

Xingyu Gao[a,1], W. Kuch[a,*], F. Offi[a], S.S. Kang[a,2], S. Imada[b], J. Kirschner[a]

[a]*Max-Planck-Institut fur Mikrostrukturphysik, Weinberg 2, D-06120 Halle, Germany*
[b]*Graduate School of Engineering Science, Osaka University, 1–3 Machikaneyama, Toyonaka 560-8531, Japan*

Abstract

In order to test the presence of interatomic multi-atom resonant photoemission (MARPE) in $3d$ magnetic ultrathin films, $2p$ photoelectron emission of various ferromagnetic $3d$ metals was studied while the excitation energy was tuned around the $L_{2,3}$ core level absorption edge of a different $3d$ metal. Both elements were in direct contact either as bilayer or as alloys to maximize this possible effect. Systems under study were Fe/Co, Fe/Ni, $Fe_{30}Ni_{70}$, Co, $Co_{90}Mn_{10}$, and $Ni_{90}Mn_{10}$, all grown as epitaxial films on Cu(001). No measurable change in intensity of the $2p$ photoemission intensities in normal emission for 45° incidence of more than 2.5–5% was found as a result of resonant excitation of neighboring atoms in any of these systems. We can thus exclude the presence of significant MARPE in these metallic systems in the present experimental geometry. This is further confirmed by the photon energy dependence of the linear magnetic dichroism in the Fe $2p$ photoemission of a Fe/Co film, which is not influenced by Co $L_{2,3}$ edge resonant absorption. © 2002 Elsevier Science B.V. All rights reserved.

Keywords: Photoelectron spectroscopy; Magnetic dichroism; Magnetic thin films

1. Introduction

The study of resonance effects in photoemission has greatly contributed to the understanding of electronic and magnetic properties of condensed matter [1–6]. Resonant photoemission conventionally implies the excitation of an atom at a resonantly

enhanced elemental core level absorption edge, and the detection of the superposition of direct photoemission and core hole decay Auger emission of the same atom. It was reported recently [7–10] that resonance effects in oxides have been observed when the excitation of the primary core hole and the emission of the detected electron take place in different neighboring atoms (interatomic multi-atom resonant photoemission, MARPE). This class of resonance effects would be a promising technique for the study of near-neighbor atomic identities, bonding, and magnetism in alloys or at interfaces. Resonant enhancements of 43% of the O $1s$ photoemission intensity in MnO [7,8] or 90% of the O KLL Auger electron intensity in Fe_2O_3 [9] have been initially

*Corresponding author. Tel.: +49-30-6392-4927; fax: +49-30-6392-4984.

E-mail address: kuch@bessy.de (W. Kuch).

[1]Present address: Department of Physics and Astronomy, Louisiana State University, Baton Rouge, LA 70803-4001, USA.
[2]Present address: University of Alabama, Materials for Information Technology, Tuscaloosa, AL 35487-0209, USA.

reported for resonant excitation at the Mn and Fe L_3 edge, respectively, and also the occurrence of a similarly significant MARPE in metallic Fe/Cr bilayers and alloys [11]. Later on, the observed effects had to be mainly attributed to experimental deficiencies related to nonlinearities in the detector response [12,13]. Nevertheless, especially at grazing incidence angles, a sizeable effect of the Mn L_3 resonant absorption on the O 1s photoemission intensity in MnO has been reported to remain even after data correction, which amounted to $> 60\%$ intensity excursion in the vicinity of the Mn L_3 edge at $10°$ grazing incidence, and $\approx 10\%$ at $30°$ incidence [12]. In O 1s photoemission from CuO, a reduction in intensity of about 20% has been found for excitation at the Cu L_3 edge [10]. No effect, however, was observed in NiO [10], LaF$_3$, Ti$_x$Nb$_{1-x}$ [14], and for adsorbed oxygen on Ni(001) [13]. A theory has been put forth that explained MARPE using retardation effects in the photon and electron interaction [15]. However, it turned out that the experimentally observed effect in MnO could be mainly explained by simply considering the X-ray optical properties of the sample [12].

The purpose of the present work is to test the presence and size of MARPE in various magnetic 3d metallic systems. We have measured the photon energy dependence of the 2p photoemission intensity of an emitter atomic species E for photon energies around the $L_{2,3}$ absorption edges of an absorber atomic species A. E and A are 3d metals in two different combinations, either as an E/A bilayer, or as an $E_x A_{1-x}$ alloy film on Cu(001). Film thicknesses were in the range of a few atomic layers. The 2p binding energy of A has thereby to be higher than that of E. We used Mn, Fe, and Co as atomic species E, and Co, Ni, and Cu as atomic species A. In none of the cases could we observe any significant variation of photoemission intensity due to interatomic resonance effects. In addition, careful measurements of the magnetic linear dichroism in Fe 2p photoemission in the vicinity of the Co $L_{2,3}$ edges have been performed in Fe/Co bilayers to test for possible interatomic resonance effects on the magnetic dichroism. Using linear magnetic dichroism instead of circular dichroism has the advantage that the sample magnetization can always be perpendicular to the light polarization axis, so that no magnetic dichroism

occurs during the absorption step. In rare earth photoemission, resonance effects in magnetic dichroism have been observed to depend on the type of resonance: while in a 'photoemission-like' resonance the dichroism is enhanced, it vanishes in the case of an 'Auger-like' resonance [6]. In both cases, a variation of intensity differences should be present, paralleling the variation in intensity. If such resonance effects were also observable in interatomic resonance, they could be used to distinguish next neighbor information not only by element, but also by the magnetism of the atoms involved. However, we find that the kinetic energy dependence of the linear magnetic dichroism at both the Fe 2$p_{1/3}$ and Fe 2$p_{2/3}$ photoemission peaks also does not reveal any sign of influence from interatomic resonance effects. The conclusion of the present work is thus that possible MARPE effects in these systems have to be smaller than 2.5–5%.

2. Experiment

The samples were all grown as ultrathin films on a Cu(001) substrate at room temperature by water-cooled electron bombardment evaporation sources. The bilayers were grown by subsequent deposition, the alloy films by co-evaporation from two different sources. The films under study were 0.5 atomic monolayers (ML) Fe/6 ML Co, 0.5 ML Fe/12 ML Ni, 3 ML Fe/8 ML Co, 6 ML Fe$_{30}$Ni$_{70}$, 8 ML Co$_{90}$Mn$_{10}$/6 ML Co, 12 ML Ni$_{90}$Mn$_{10}$, and 0.5 ML Co. The pressure during evaporation could be kept below 2×10^{-8} Pa. The thickness of the films was controlled by medium energy electron diffraction (MEED) intensity oscillations during evaporation. Before deposition of the binary alloy films the evaporation rates of both evaporators were first calibrated separately by MEED. No impurities on the sample before and after deposition of the films could be detected using Auger electron spectroscopy (AES). AES was also used to reconfirm the film thickness and alloy composition.

The photoemission experiments were performed at the UE 56-I PGM beamline of the Berlin synchrotron radiation facility BESSY II using linearly p-polarized light. The light was incident under $45°$ in the [110] azimuth of the substrate, and electrons were

detected at normal emission. Photoelectron energy spectra were collected using a commercial hemispherical electron energy analyzer (HA 150, VSW Scientific Instruments Ltd.) with multichannel detection. Details of the experimental set-up have already been described elsewhere [16]. For the present measurements the pass energy of the analyzer was set to 44 eV, which corresponds to an energy resolution of 0.6 eV. The photon energy resolution was selected as $E/\Delta E = 1500$, so that the overall experimental resolution was between 0.8 and 0.9 eV. Variations of the incident photon flux have been taken into account by dividing the measured intensity by the photocurrent of a gold grid located behind the last optical element. For the magnetic dichroism measurements, photoemission spectra were recorded for two opposite directions of the sample magnetization perpendicular to the plane defined by light incidence and sample normal. Magnetization reversal was achieved by discharging a capacitor through a coreless coil close to the sample position.

3. Results and discussion

Fig. 1(a) shows a series of Fe $2p$ photoemission spectra of 0.5 ML Fe/6 ML Co. The displayed spectra have been obtained by averaging spectra for opposite in-plane magnetization direction perpendicular to the light incidence. The photon energy was varied in the vicinity of the Co $L_{2,3}$ excitation threshold, as labeled at the right-hand side of each spectrum. Individual spectra are vertically offset by a
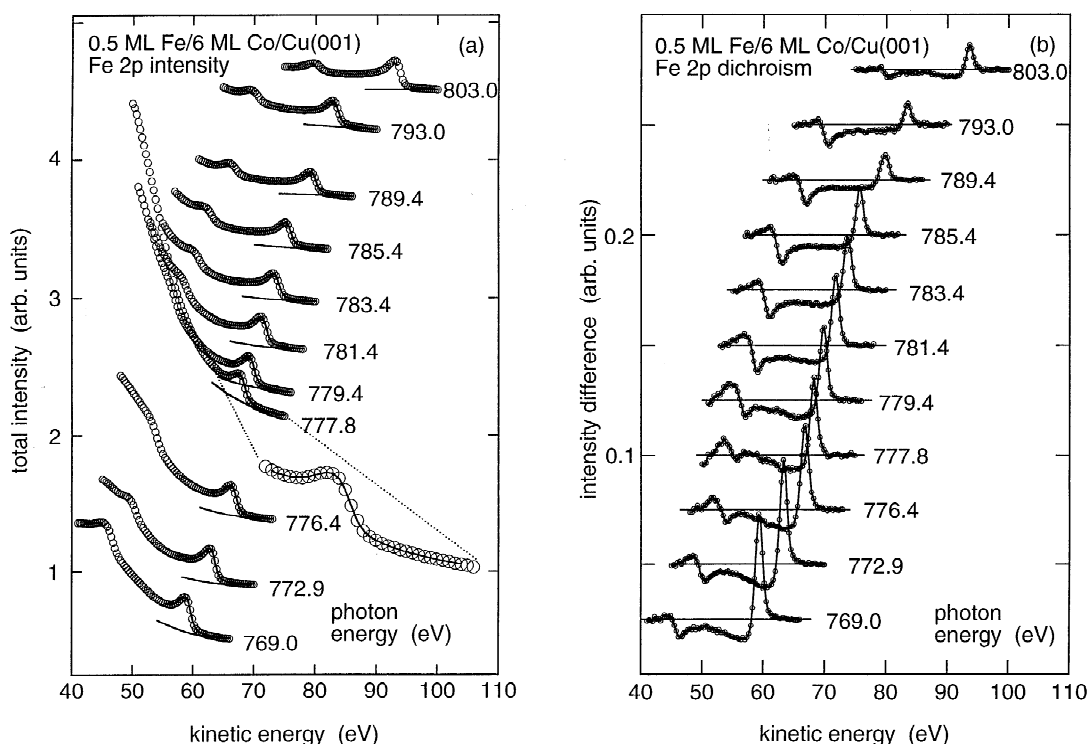

Fig. 1. (a) Fe $2p$ photoemission spectra of 0.5 ML Fe/6 ML Co/Cu(001) at different photon energies around the Co $L_{2,3}$ absorption edges as labeled in the figure. Spectra are vertically offset by a constant amount with respect to each other for clarity. Solid lines show the result of constant shape fits using the spectrum at 803 eV photon energy as a template, and the polynomial approximating the background at the Fe $2p_{3/2}$ peak. A zoom-in of the spectrum at Co L_3 resonant excitation (777.8 eV photon energy) is also shown; (b) The corresponding Fe $2p$ linear magnetic dichroism spectra, obtained as intensity difference of photoelectron spectra for opposite sample magnetization in the film plane, perpendicular to the light incidence. Spectra are vertically offset by a constant amount with respect to each other for clarity. Note the different vertical scale in (a) and (b).

constant shift with respect to each other for clarity. Open circles represent the experimental data. The Fe $2p_{3/2}$ peak, which is shifted towards higher kinetic energy with increasing photon energy, is clearly seen in the spectra. The sometimes rather weak Fe $2p_{1/2}$ peak can also be distinguished at 13 eV lower kinetic energy. The spectra shown in Fig. 1(a) are superimposed on a background consisting of contributions from both secondary electrons as well as Fe $M_{2,3}VV$ (centered at about 47 eV), and Co $M_{2,3}VV$ (centered at about 53 eV) Auger electrons. The secondary electrons and the Co Auger electrons are strongly enhanced at Co L_3 resonant absorption, as is seen from the spectrum at 777.8 eV photon energy. It is therefore essentially important to find a systematic way to precisely subtract this background in order to study the photon energy dependence of the Fe $2p$ photoemission intensity. In order to do so, we have chosen to perform constant shape fits. The photoelectron spectrum obtained by the highest photon energy excitation of each film minus a constant background was used as a template spectrum to fit all other spectra of the same film in an energy range of 10 eV around the $2p_{3/2}$ photoemission peak. In this fit range we can approximate the background contribution by a polynomial of second-order in the kinetic energy. Fit parameters for the constant shape fit are then the three coefficients describing the polynomial background, and a scaling factor that is needed to scale the template curve in order to match the individual curves. The latter represents the Fe $2p_{3/2}$ relative photoemission intensity. In this way, all the spectra in Fig. 1(a) could be fitted well by the template spectrum, which in this case was the spectrum acquired at 803 eV photon energy. The results of the fits are shown as solid lines within the experimental data points in Fig. 1(a). Excellent agreement is achieved for all spectra. For better visibility a zoom-in of the spectrum at Co L_3 resonant excitation (777.8 eV photon energy) is shown. This spectrum exhibits the largest contribution from inelastic background and is thus the most difficult to fit. Also plotted in Fig. 1(a) are the polynomial background curves. The scaling factor from the constant shape fit is later used to represent the relative photoemission intensity.

In Fig. 1(b) the corresponding series of magnetic dichroism spectra, i.e. the photoemission intensity difference that occurs upon reversal of the sample magnetization, is presented. Again, the spectra are vertically offset for clarity. The horizontal solid lines represent the zero of each spectrum. Note that the vertical axis is scaled up by a factor of about 17 compared to Fig. 1(a). All of the presented difference spectra show the typical 'minus/plus' and 'plus/minus' excursions at the Fe $2p_{3/2}$ and the Fe $2p_{1/2}$ levels, respectively. The shape of the spectra agrees well with previously published data [16–18]. A strong photon energy dependence of the size of the dichroism is clearly seen. It is different for the $2p_{1/2}$ and the $2p_{3/2}$ line. Whereas the former shows maximum dichroism around 780 eV photon energy, the latter is maximal for the lowest photon energies used here. This different behavior of the $2p_{1/2}$ and the $2p_{3/2}$ dichroism as a function of photon energy consequently also influences to some extent the shape of the difference curves in between the $2p_{1/2}$ and the $2p_{3/2}$ photoemission lines. To access the size of the magnetic dichroism, the peak-to-peak intensity differences at the Fe $2p_{3/2}$ and Fe $2p_{1/2}$ lines are used in the following, which are robust against small baseline deviations.

The photoemission intensity from Fig. 1(a) as a function of photon energy as determined from the scaling factor of the constant shape fits is depicted in Fig. 2(a). Also shown as a solid line is the absorption spectrum of the same sample, recorded using the sample current. The absorption spectrum shows peaks due to Co L_3 and L_2 resonant excitation at photon energies of 778 and 793 eV, respectively. Fig. 2(b) shows the photon energy dependence of the Fe $2p_{3/2}$ dichroism (solid symbols) and the Fe $2p_{1/2}$ dichroism (open symbols) from Fig. 1(b). Also here the absorption spectrum is reproduced as a solid line.

The intensity in Fig. 2(a) varies smoothly with photon energy as indicated by the dashed line, which serves as a guide to the eye. This intensity variation with photon energy is governed by the transmission of the electron optics of the detector, which is roughly described by a $1/E_{kin}$ dependence, the variation of atomic Fe $2p$ photoemission cross-section including angle-dependent interference effects [19], the absorption cross-section of the gold grid used for normalization, and photoelectron diffraction effects due to the crystallinity of the sample. The Fe $2p_{3/2}$ photoemission intensity as a function of photon
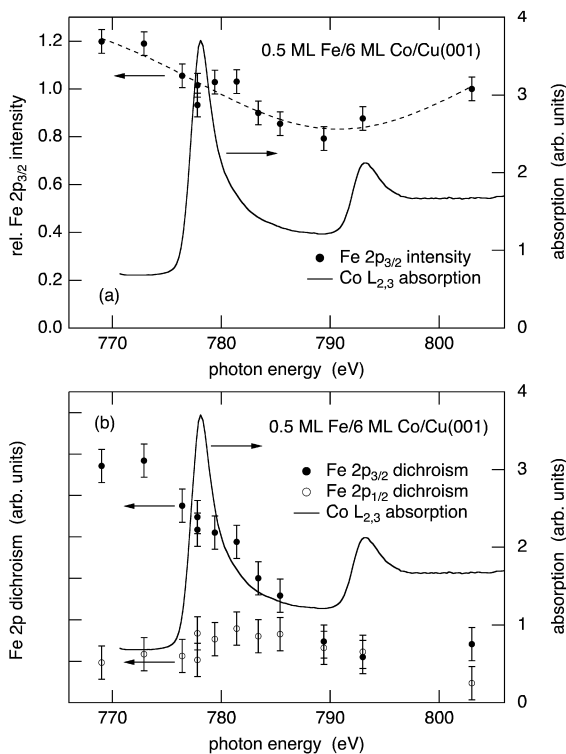
Fig. 2. (a) Fe $2p_{3/2}$ photoemission intensity of the spectra of Fig. 1 (a) as a function of photon energy for 0.5 ML Fe/6 ML Co/Cu(001) (symbols, left-hand scale), and absorption (solid line, right-hand scale). The dashed line serves as a guide to the eye. No influence of the resonant Co $L_{2,3}$ absorption on the photoemission intensity is observed; (b) Fe $2p_{3/2}$ and $2p_{1/2}$ linear magnetic peak-to-peak dichroism (solid and open symbols, respectively, left-hand scale) as a function of photon energy. Again the absorption spectrum is depicted as a solid line (right-hand scale). Also here no influence of the resonant Co $L_{2,3}$ absorption on the magnetic dichroism is observed.

energy has no correlation with the Co absorption spectrum, and is not significantly influenced at the Co L_3 maximum, as would be expected from inter-atomic resonance effects [7–9], within the experimental error bars of about 5%. Thus, from this behavior of the photoemission intensity we can conclude that there is no significant MARPE at the Fe/Co interface in that sample.

The intensity differences, i.e. the dichroisms, exhibit a stronger but smooth variation with photon energy (cf. Fig. 2(b)). No sudden variations in Fig. 2(b) related to the Co absorption edges are present, so that we can rule out an influence of MARPE on

magnetic dichroism. In order to understand the origin of the different photon energy dependences of the magnetic dichroism at the Fe $2p_{3/2}$ and $2p_{1/2}$ peaks, Fig. 3 shows a plot of the dichroism as a function of photoelectron kinetic energy. Again, solid and open symbols correspond to $2p_{3/2}$ and $2p_{1/2}$ dichroism, respectively. The solid lines represent a smooth polynomial function which serves as a guide to the eye. Note that both solid lines are identical except for a constant scaling factor. It is obvious from this plot that the Fe dichroism at both peaks follows the same kinetic energy dependence. This points either towards an intrinsic kinetic energy dependence of the transition matrix elements the interference of which is leading to magnetic linear dichroism, or towards the influence of photoelectron diffraction effects. In Ref. [19], van der Laan has presented the kinetic energy dependence of Fe $2p$ and $3p$ linear dichroism from Hartree–Fock calculations. However, the calculated Fe $2p$ dichroism changes very little in the present kinetic energy range. We conjecture therefore that photoelectron diffraction effects, which are exceptionally kinetic-energy-dependent, may dominate the observed kinetic energy dependence of the
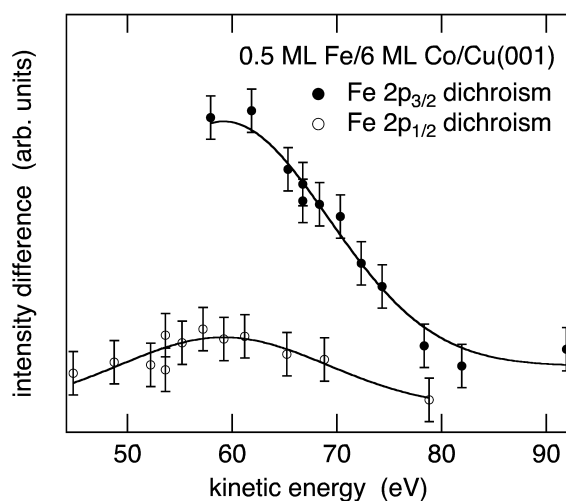

Fig. 3. Fe $2p_{3/2}$ and $2p_{1/2}$ linear magnetic peak-to-peak dichroism (solid and open symbols, respectively) as in Fig. 2(b), but plotted here as a function of photoelectron kinetic energy. The solid lines are guides to the eye. They result from the same smooth polynomial, scaled by different constant factors to demonstrate that both Fe $2p_{3/2}$ and $2p_{1/2}$ dichroisms follow the same kinetic energy dependence.

linear magnetic dichroism. Very similar kinetic energy dependence of MLDAD in this energy range has also been observed for Fe $3p$ photoemission [20,21]. In particular, in Ref. [21] it was found that the strong variations of the MLDAD around 50–150 eV are not observed when the sample is a polycrystalline Fe film. The authors arrive at the same conclusion as we do, that the observed strong modulations of the dichroism are due to photoelectron diffraction effects. The slightly different kinetic energy for the maximum dichroism in the present experiment (about 60 eV) and in Ref. [21] (about 70 eV) can easily be explained by the different lattice parameter of f.c.c. and b.c.c. Fe(001). The presence of dominant photoelectron diffraction effects in MLDAD implies also immediately that the contribution of these effects to the observed energy dependence of the photoemission intensity (cf. Fig. 2(a)) must also be sizeable.

Fig. 4 reports the Fe $2p_{3/2}$ photoemission intensity as a function of photon energy around the Ni $L_{2,3}$ edges for three different films: 0.5 ML Fe/12 ML Ni (solid circles), 6 ML $Fe_{30}Ni_{70}$ (squares), and 3 ML Fe/8 ML Co (open circles). The last film does not contain Ni, and is just used as a reference to demonstrate the photon energy dependence of the Fe $2p_{3/2}$ photoemission intensity in the same photon energy interval without resonant excitation. The solid
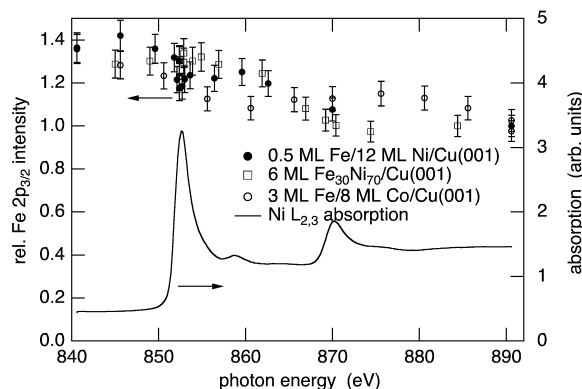

Fig. 4. Fe $2p_{3/2}$ photoemission intensity as a function of photon energy. Solid circles: 0.5 ML Fe/12 ML Ni/Cu(001), squares: 6 ML $Fe_{30}Ni_{70}$/Cu(001), open circles: 3 ML Fe/8 ML Co/Cu(001). The solid line is the absorption curve of 0.5 ML Fe/12 ML Ni/Cu(001), showing the Ni $L_{2,3}$ absorption edges. No influence of the resonant Ni $L_{2,3}$ absorption on the photoemission intensity is observed.

line is the absorption curve of 0.5 ML Fe/12 ML Ni, showing the Ni L_3 and L_2 peaks. Both the Fe/Ni and $Fe_{30}Ni_{70}$ films clearly show no sign of MARPE at the Ni resonant absorption, their photon energy dependences being very similar to each other around the Ni L_3 edge and also to that of the Fe/Co film. The slightly different photon energy dependence around the L_2 edge may be explained by different photoelectron diffraction effects or different extended absorption fine structure in the three different films with different thicknesses.

Fig. 5 shows the photon energy dependences of the Mn $2p_{3/2}$ photoemission intensity of 8 ML $Co_{90}Mn_{10}$/6 ML Co in the photon energy range of the Co $L_{2,3}$ edges in panel (a), and of 12 ML $Ni_{90}Mn_{10}$ in the photon energy range of the Ni $L_{2,3}$ edges in panel (b). Panel (c) shows the photon energy dependence of the Co $2p_{3/2}$ photoemission intensity of 0.5 ML Co/Cu(001) in the photon energy range of the Cu $L_{2,3}$ edges. The solid lines are the absorption curves of the respective samples. Only a very smooth photon energy dependence of the Mn $2p_{3/2}$ and Co $2p_{3/2}$ photoemission intensity is observed, with clearly no sign of any resonant behavior. In $Ni_{90}Mn_{10}$ and Co/Cu(001) this can even be stated within less than 2.5% error.

For all the above metallic films, the photon energy dependence of the photoemission intensity shows no evidence for the existence of a significant MARPE effect either in alloys or from interfaces. One reason for this very small effect could be related to the fact that direct recombination processes are weak in the delocalized $3d$ metals [22,23]. Jensen et al. used a hopping process to explain the enhanced core-valence-valence Auger process of the surface in Ta(001) [24]. Thereby the hopping rate depends on the convolution of the occupied layer-resolved density of states of both involved atoms at the difference energy of the two states. Whereas for the hopping from Ta bulk to surface atoms with an energy difference of just 0.74 eV a sizeable effect results, this model would yield close to zero effect for the case of much more energetically separated core levels of different elements. The absence of significant interatomic resonance in $3d$ metals may also be simply related to the absence of normal intra-atomic resonance in these systems, a topic that is controversially discussed in literature [4,25–30]. A picture
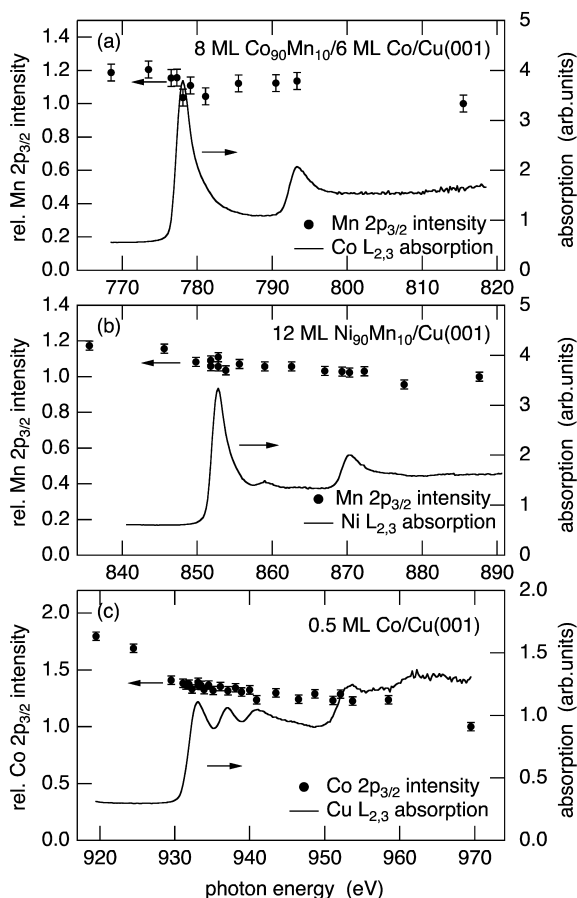
Fig. 5. (a) Mn $2p_{3/2}$ photoemission intensity of 8 ML $Co_{90}Mn_{10}/$ 6 ML Co/Cu(001) as a function of photon energy in the range of the Co $L_{2,3}$ edges. (b) Mn $2p_{3/2}$ photoemission intensity of 12 ML $Ni_{90}Mn_{10}/Cu(001)$ as a function of photon energy in the range of the Ni $L_{2,3}$ edges. (c) Co $2p_{3/2}$ photoemission intensity of 0.5 ML Co/Cu(001) as a function of photon energy in the range of the Cu $L_{2,3}$ edges. The solid lines are the absorption curves of the same samples. No influence of the resonant absorption on the Mn or Co photoemission intensity is observed.

of MARPE in which it is simply related to the variation of the optical constants in the vicinity of core level absorption edges is emerging from theoretical simulations of MnO MARPE of Ref. [12]. The variation of the X-ray refractive index is related to the absorption intensity, which in turn depends on the number of unoccupied valence states [31]. Since the number of $3d$ holes is much higher in MnO compared to the late $3d$ metals Co, Ni, and Cu, which were used in the present study as absorbers,

the effect expected in this picture should thus be much weaker compared to the Mn L_3 edge of MnO.

4. Summary and conclusion

No significant photoemission intensity variation due to interatomic resonance effects in $2p$ core-level photoemission of $3d$ metals for resonant excitation of the $L_{2,3}$ edge of a different $3d$ metal was observed in any of the combinations of $3d$ metals used in our study in the present experimental geometry. While the study of magnetic linear dichroism in Fe/Co revealed a strong kinetic energy dependence, no indication for the existence of interatomic resonance in magnetic dichroism is observed. We therefore think that generally MARPE is very weak in the late $3d$ metals. It will consequently be extremely difficult to use MARPE to detect next neighbor chemical identities. As a technique for the study of alloys or interface structure in these systems, MARPE is therefore clearly not well suited. Further extensive studies, also involving the light incidence angle dependence, will be necessary to elucidate the exact mechanisms which may lead to MARPE effects in photoemission of less than 2.5–5% in these $3d$ metal systems.

References

[1] C. Guillot, Y. Ballu, J. Paigné, J. Lecante, K.P. Jain, P. Thiry, R. Pinchaux, Y. Pétroff, L.M. Falicov, Phys. Rev. Lett. 39 (1977) 1632.
[2] D. Chandesris, J. Lecante, Y. Pétroff, Phys. Rev. B 27 (1983) 2630.
[3] B.T. Thole, H.A. Dürr, G. van der Laan, Phys. Lett. 74 (1995) 2371.
[4] C. Laubschat, J. Electron Spectrosc. Relat. Phenom. 96 (1998) 127.
[5] S. Suga, A. Kimura, T. Matsushita, A. Sekiyama, S. Imada,

K. Mamiya, A. Fujimori, H. Takahashi, N. Mori, Phys. Rev. B 60 (1999) 5049.

[6] S.R. Mishra, T.R. Cummins, G.D. Waddill, W.J. Gammon, G. van der Laan, K.W. Goodman, J.G. Tobin, J. Vac. Sci. Technol. A 17 (1999) 1313.

[7] A. Kay, E. Arenholz, B.S. Mun, F.J. García de Abajo, C.S. Fadley, R. Denecke, Z. Hussain, M.A. Van Hove, Science 281 (1998) 679.

[8] A. Kay, E. Arenholz, B.S. Mun, F.J. García de Abajo, C.S. Fadley, R. Denecke, Z. Hussain, M.A. Van Hove, J. Electron Spectrosc. Relat. Phenom. 101–103 (1999) 647.

[9] E. Arenholz, A.W. Kay, C.S. Fadley, M.M. Grush, T.A. Callcott, D.L. Ederer, C. Heske, Z. Hussain, Phys. Rev. B 61 (2000) 7183.

[10] M. Finazzi, G. Ghiringhelli, O. Tjernberg, L. Duò, A. Tagliaferri, P. Ohresser, N.B. Brookes, Phys. Rev. B 62 (2000) R16215.

[11] E. Arenholz, A.W. Kay, C.S. Fadley, Talk DG-11 presented at 44th Annual Conference on Magnetism and Magnetic Materials, San Jose, CA, USA, Nov. 15–18, 1999.

[12] A. Kay, F.J. García de Abajo, S.H. Yang, E. Arenholz, B.S. Mun, N. Mannella, Z. Hussain, M.A. Van Hove, C.S. Fadley, Phys. Rev. B 63 (2001) 115119.

[13] D. Nordlund, M.G. Garnier, N. Witkowski, R. Denecke, A. Nilsson, M. Nagasono, N. Mårtensson, A. Föhlisch, Phys. Rev. B 63 (2001) 121402.

[14] M. Moewes, E.Z. Kurmaev, D.L. Ederer, T.A. Callcott, Phys. Rev. B 62 (2000) 15427.

[15] F.J. García de Abajo, C.S. Fadley, M.A. Van Hove, Phys. Rev. Lett. 82 (1999) 4126.

[16] X. Gao, M. Salvietti, W. Kuch, C.M. Schneider, J. Kirschner, Phys. Rev. B 58 (1998) 15426.

[17] C.M. Schneider, U. Pracht, W. Kuch, A. Chassé, J. Kirschner, Phys. Rev. B 54 (1996) R15618.

[18] X. Gao, M. Salvietti, W. Kuch, C.M. Schneider, J. Kirschner, J. Electron Spectrosc. Relat. Phenom. 113 (2001) 137.

[19] G. van der Laan, Phys. Rev. B 55 (1997) 3656.

[20] J. Bansmann, L. Lu, K.H. Meiwes-Broer, T. Schlathölter, J. Braun, Phys. Rev. B 60 (1999) 13860.

[21] G. Panaccione, F. Sirotti, G. Rossi, Solid State Commun. 113 (2000) 373.

[22] M. Finazzi, N.B. Brookes, F.M.F. de Groot, Phys. Rev. B 59 (1999) 9933.

[23] M. Finazzi, G. Ghiringhelli, O. Tjernberg, P. Ohresser, N.B. Brookes, Phys. Rev. B 61 (2000) 4629.

[24] E. Jensen, R.A. Bartynski, M. Weinert, S.L. Hulbert, E.D. Johnson, R.F. Garrett, Phys. Rev. B 41 (1990) 12468.

[25] M.F. López, A. Höhr, C. Laubschat, M. Domke, G. Kaindl, Europhys. Lett. 20 (1992) 357.

[26] A. Gutiérrez, M.F. López, Phys. Rev. B 56 (1997) 1111.

[27] L.H. Tjeng, C.T. Chen, J. Chijsen, P. Rudolf, F. Sette, Phys. Rev. Lett. 67 (1991) 501.

[28] M. Weinelt, A. Nilsson, M. Magnuson, T. Wiell, N. Wassdahl, O. Karis, A. Föhlisch, N. Mårtensson, J. Stöhr, M. Samant, Phys. Rev. Lett. 78 (1997) 967.

[29] M. Magnuson, N. Wassdahl, A. Nilsson, A. Föhlisch, J. Nordgren, N. Mårtensson, Phys. Rev. B 58 (1998) 3677.

[30] M. Magnuson, A. Nilsson, M. Weinelt, N. Mårtensson, Phys. Rev. B 60 (1999) 2436.

[31] J. Stöhr, J. Electron Spectrosc. Relat. Phenom. 75 (1995) 253.